

The Use of Outcrops on the Catalonian Coastal Ranges (Spain) as Analogue for Deep Geothermal Reservoir Characterization in the Upper Rhine Graben (France).

Lionel Bertrand¹, Yves Géraud¹, Marc Diraison², Edouard Le Garzic, Joachim Place

1 GeoRessources, UMR 7359 Université de Lorraine/ENSG, 2 rue du Doyen Marcel Roubault, Vandoeuvre-les-Nancy Cedex 54518, France

2 Institut de Physique du Globe (IPG), UMR 7516 CNRS-Université de Strasbourg/EOST, 5 rue René Descartes, Strasbourg Cedex 67084, France

lionel.bertrand@univ-lorraine.fr

Keywords: graben basement, fractures, outcrop analogue, reservoir model.

ABSTRACT

Graben structures are extensively prospected as high enthalpy geothermal targets. The West European rift system started during the Oligocene and stopped their extension during the Miocene. In this graben, the existence of particularly high thermal gradient spots allows to consider the opportunity to develop different deep geothermal energy projects. These projects aim to exploit the graben basement and the interface with the overlapping sediments.

Due to the poor matrix permeability of these rocks, the fluid flow in these reservoirs is mainly controlled by the natural fracture and fault network and associated weathered materials. Unfortunately, the fracture and fault pattern at reservoir scale in the basement is not well known and difficult to characterize with the actual geophysical tools. The use of analogue outcrops is therefore an important tool for improving the reservoir characterization.

This study presents a multiscale analysis of the basement in the Catalonian Coastal Ranges that outcrops at the shoulder of the West European Rift in north-east Spain. First, we combined satellite images, field studies and laboratory measurements in order to define the fault and fracture network at large scale with the characterization of structural parameters, e.g., length, orientation. As a result, we built a reservoir model composed by blocks of different thickness and length depending on the fault boundaries. Blocks and faults were populated with their reservoir or matrix porosity. The second step was to compare these geometrical properties acquired from outcrops with data from the well-known Soultz-sous-Forêt EGS site to contribute to the understanding of fluid circulation in the basement reservoir locally and regionally within the graben.

1. INTRODUCTION

To generate electricity from geothermal energy, the minimal temperature of the geothermal fluids required is around 200°C. In non-volcanic areas, this temperature implies an exploitation depth at around 5000 m. In classical sedimentary basins, this depth corresponds to reservoirs at the interface between the basement and overlying sediments, and in so-called fractured basement reservoirs. The flow in this basement is mainly controlled by fault and fracture networks due to the generally low matrix porosity and permeability. Unfortunately, the structure of the basement is not well known, and thus, the prediction of the flow paths for a geothermal production is difficult. Furthermore, for the entire comprehension of the flow system, it is necessary to know the fracture parameters, e.g. density, orientation, lengths, at different scales, from the local borehole to the regional seismic data. But there is a lack of visualization between these two scale boundaries and the fractures are, therefore, not well known at the reservoir scale. The study of outcropping analogues of buried reservoirs is a key tool for the characterization of the fracture network at reservoir scale in order to make the connection between seismic and borehole data.

Due to the geothermal gradient particularly high the Upper Rhine Graben, several industrial projects for the exploitation of the geothermal fluids are under development. The study presented here aims to enhance the knowledge of the fracture network in the graben basement and, more generally, of basement reservoirs in extensional regions. Two areas will be compared: The Catalonian Coastal Ranges, where the basement outcrops at the shoulders of the Mediterranean Basin, and the Upper Rhine Graben buried basement with the help of Soultz-sous-foret EGS data. The basements have the same structural heritage: formed during the Hercynian orogen and mainly deformed by the opening of the West European Rift during the Oligocene, allowing the comparison between the two locations. A multiscale analysis between the regional scale and the hand sample and core scale will be made, with fracture analysis and petrophysical measurements, in order to define general scaling laws in fractured basement within this geological setting.

2. GEOLOGICAL CONTEXT

The West European Rift is a first class target for geothermal exploitation in deep reservoirs. Even though this rifting has been rapidly aborted, it has significantly thinned the continental crust allowing an upwelling of the mantle. This crustal setting produced a high geothermal gradient and local anomalies allowing the development of several industrial projects for the exploitation of hot fluids (Fig. 1a). Nevertheless, in order to obtain the 200°C for electricity generation, the reservoir targets are located in the Hercynian basement of the graben where the structures are largely influenced by the Hercynian orogeny.

2.1 The West European Rift

The West European Rift is the result of a wide rifting event that took place in Western Europe in response to the collision between the European and the African plates. This rifting induced the formation of a series of grabens propagating from the Rhine Graben

towards the south and north beginning at the end of the Eocene. To the south, the deformation moved from the Rhine Graben to the Bresse Graben, and then to the Lyon Gulf, controlling the NE-SW Mediterranean coast of southern France and north-east Spain. These basins were progressively filled with sediments until the rifting stopped at the beginning of the Miocene (Fig. 1b).

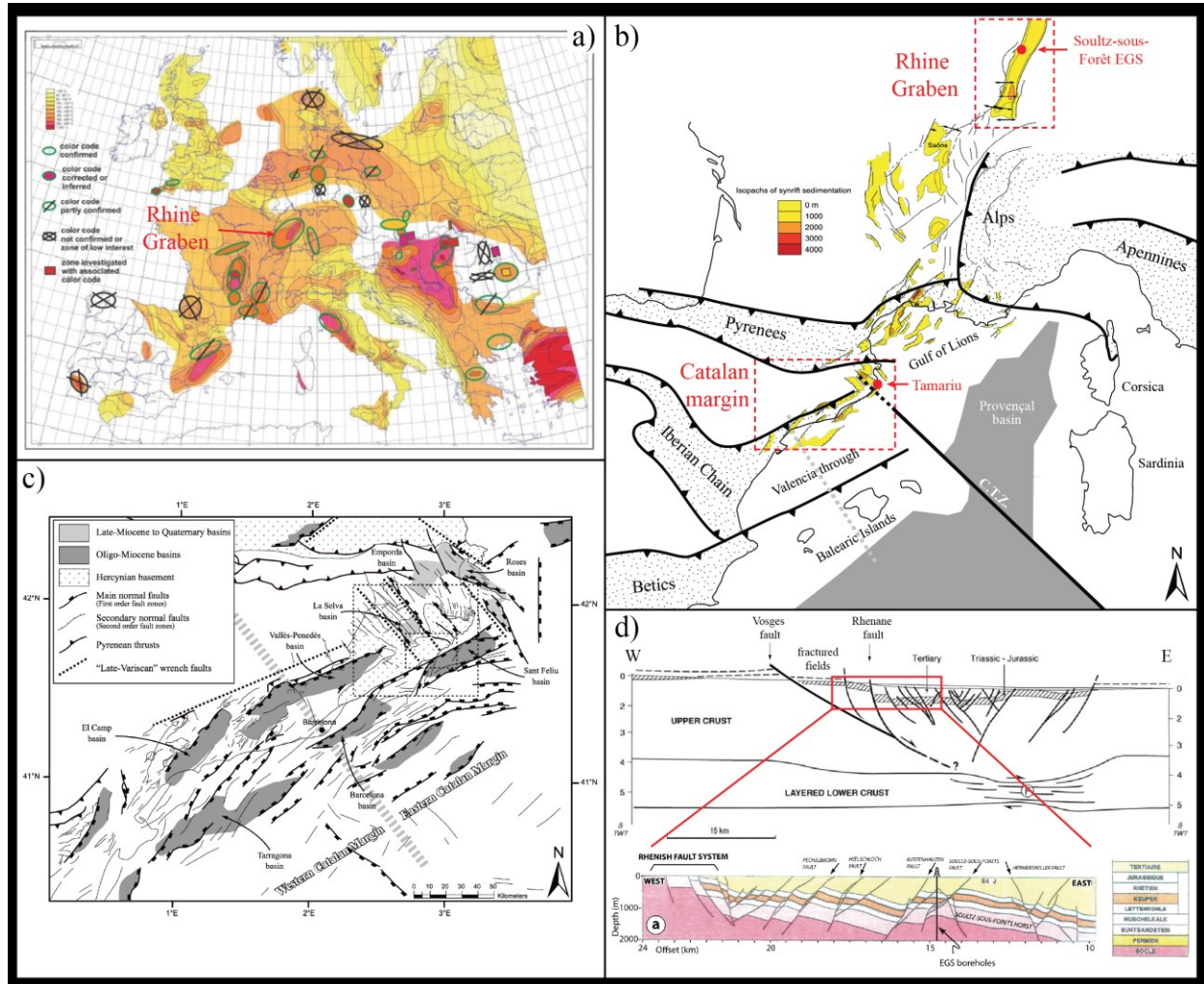


Figure 1: a) Temperatures and analyses of heat sources in Europe at 5000 m depth by Genter et al. (2003) modified from Haenel et al. (1980), b) simplified map of the southern propagation of the West European Rift with syn-rift sediments thickness, modified from Séanne (1999), c) structural map of the Catalonian Coastal Ranges by Roca et al. (1999), d) interpretation and schematic view of ECORS seismic lines cross-cutting the URG, modified from Cautru (1989) and Brun et al. (1991).

The Catalonian Coastal Ranges (CCR) are a part of the Catalan Margin in the NE of Spain at the southern prolongation of the rift system. They are composed of a series of tilted blocks, with NE-SW elongation and structured by approximately N050°E faults (Fig. 1c). The basins are filled by Neogene sediments and the Hercynian basement outcrops at the heads of the tilted blocks. In addition to the generally NE-SW faults, there are NW-SE faults in the northern part of the CCR that are linked to the onshore propagation of the Catalonian Transform Fault Zone (CTZ). In some parts of the margin, natural heat source with an equivalent temperature of natural fluids in the Rhine Graben (see below) have been identified.

The Upper Rhine Graben is a collapsing graben located at the frontier between France and Germany, elongated approximately in the N020°E direction, with a length of 300 km and 30 km wide. The deformation that induces the graben is divided in two steps: a first simple opening stage with an E-W extension, and a second step of strike-slip motion along the N020°E faults induced by NNW-SSE compression. This last stage is active at present. Locally, the graben is divided in a series of tilted blocks deepening progressively from the bordering faults to the center of the basin (Fig. 1d).

The two areas expose the same structure with a series of tilted blocks filled or partially filled by sediments, and a shift of the bordering faults from N020°E to N050°E. This shift is the consequence of the structural heritage of the Hercynian orogeny that largely controls the basement structures.

2.2 The Hercynian heritage

The basement of the Rhine Graben and the Catalan Margin is formed of rocks linked to the Hercynian orogeny. In the areas of interest, they are mainly composed of metasediments and large-scale magmatism with Proterozoic to Carboniferous ages. In this part of Europe, The Hercynian basement is composed of a series of microplates separated from the Gondwana Plate by different

oceanization stages before the general shortening and the closing of the basins between the Laurensia and Gondwana plates (Skrzypek, 2011; Thabaud, 2012). The shortening direction is regionally N-S, forming large scale N050°E and N130°E trusts between the different parts of the orogeny. At the end of the orogeny, the collapse of the Hercynian chain is associated with NNE-SSW and NNW-SSE large-scale strike-slip fault zones (Arthaud and Matte, 1975).

All these structures have largely influenced the post carboniferous deformations, from the late Permian orogenic extensional phase, when the basement was uplifted to the surface and eroded, until the West European rifting event. Thus, the reactivation of the Hercynian trusts and strike-slips have a large impact on the structure of the basement and overlying sediments, namely on the morphology of the Oligocene basins with the shift of their orientation from the URG to the south.

3. THE CATALONIAN COASTAL RANGES

3.1 Regional scale

The fault network of the Catalonian Coastal Ranges has been studied at different scales, from the whole Catalan Margin to the scale of a single horst, with help of satellite images at different resolution and field observations (Le Garzic, 2010). By mapping different fault parameters including width, resolution, orientation, length and spacing distribution, the faults have been characterized at different scales of observation.

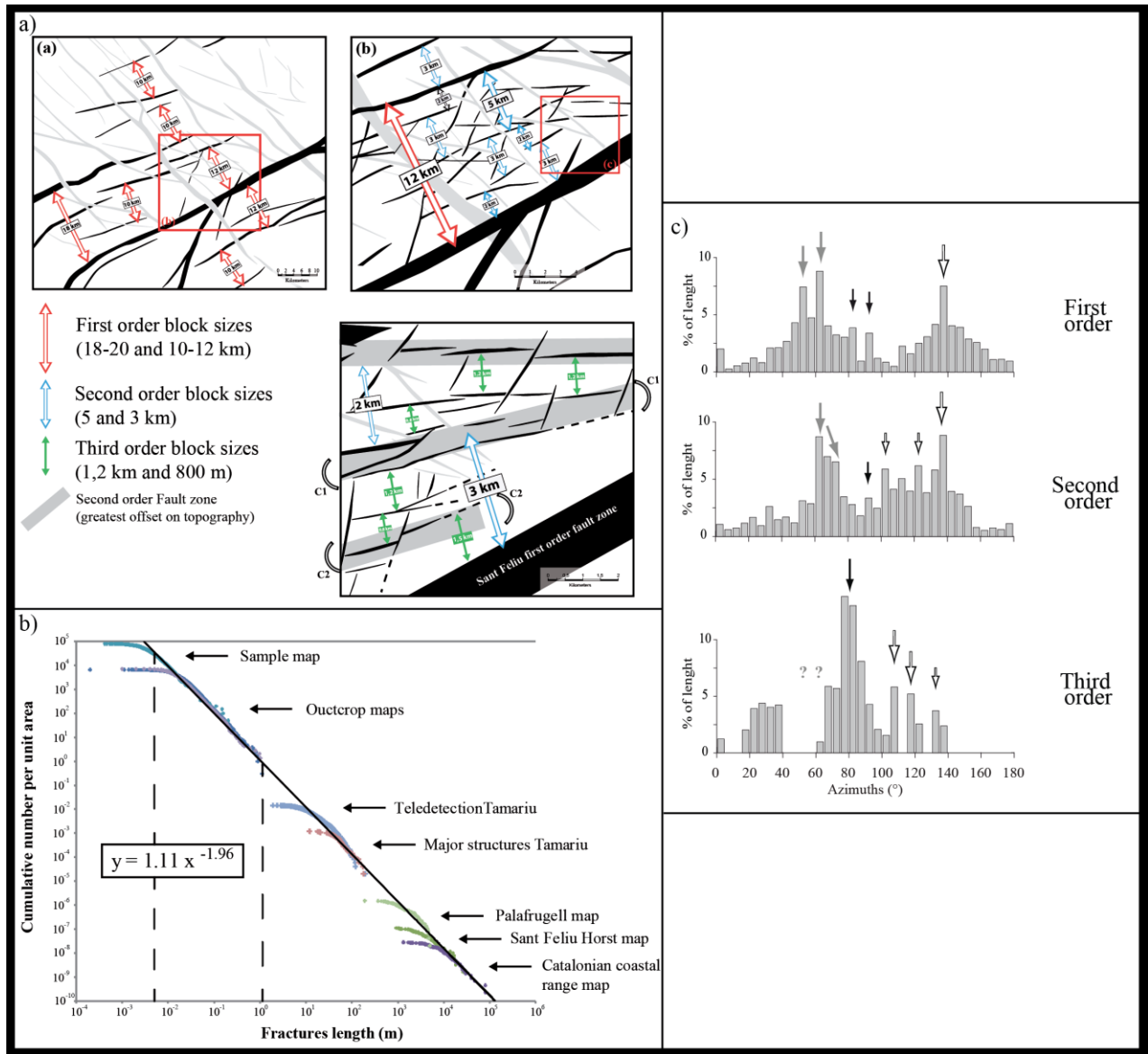


Figure 2: a) Schematic synthesis of faults organization in three orders of blocks of the Catalan Margin by Le Garzic (2010), b) cumulative length distribution of faults and fractures on the CCR from regional to centimeter scale by Bertrand et al (in review), c) orientation of faults at each scale of structural block by Le Garzic (2010).

With these data, four orders of faults are defined: 1) the first order is composed of the lithospheric and crustal faults, such as basin borders or suture zones, where most part of the deformation is located, and that have characteristic lengths of hundred kilometres and spacing of 10 to 20km. 2) The second order faults propagate in the upper crust and are visible at the seismic scale. They accommodate large depocenters for sediments and merge on first order faults in depth. They are typically 20-30 km in length and

have 3 to 5 km spacing. 3) The third order faults are those at the lower limit of detection of the classic seismic lines and are better visible in outcrops, their typical length is around 10 km with spacing around 1 km. 4) The fourth order faults are less than 1 km in length. In addition, the fault system in the CCR is divided in two systems (Roca et al., 1999): 1) N000°E to N100°E trending faults that are Hercynian herited faults reactivated during the tectonic events before and during the West European rifting phase, and 2) N100°E to N150°E trending faults linked to the Catalonian Transform Zone (CTZ) that extends in the onshore part of the Catalan Margin.

With this multiscale analysis we have access to fault parameters such as length, orientation and density on the whole range of scales from the regional margin scale to hand samples taken on Tamariu's outcrop (see next section). The fracture length data mapped at different scales and plotted in cumulative frequency normalized per area unit against fracture length is shown in Fig. 2c. Outside the biases linked to the map resolution and width (censoring and truncation) all data show a power-law distribution with an exponent near -2. This highlights that the fault system is self-similar, i.e. the behavior of the fault length is independent of the scale of observation, from the first order fault dividing the Catalan Margin to the small centimeter fractures visible on a hand sample. In contrast to the length, the faults orientation shows different trends between different scales. For the first system of faults, the first and second order faults are mainly rifting faults and intra-block oblique faults (grey arrows, Fig. 2d) with only few inherited Hercynian N090°E faults, while these inherited directions are largely dominant for the third order faults (black arrows, Fig 2d). For the second system linked to the CTZ, a main fault direction is visible on the first order faults suggesting an apparently simple fault system but it becomes more complex at the second and third orders with different slightly oblique directions (white arrows, Fig. 2d).

3.2 Reservoir scale

The typical scale acting in fractured reservoirs is third order, with blocks and faults using smaller flow paths to make the connection between the bordering faults of the blocks. Tamariu outcrop represents a section in one of these third order blocks of approximately 1 km length outcropping along the Mediterranean coast (Fig. 3a). This block is divided in four fourth order blocks by E-W faults and in these blocks there is a fracture pattern partly filled by carbonates. These carbonates have been associated with hydrothermal fluids circulation with temperatures between 168 and 193°C (Place, 2010). With these conditions, they are good markers of paleogeothermal circulation in the fracture network of the granite.

We have analyzed the southern end of block 3 which was the best exposed on the coast and the flattest, allowing a good statistical analysis of the fractures. Different scales were investigated: after locating the main fractures, i.e. those longer than 10 m, we used scan line measurements in order to determine the density, orientation and length of fractures and carbonate veins from decimeters to ten meter length. We took photographs in order to characterize the fractures and veins distribution with lengths from centimeters to one meter. Finally, we took hand samples in order to analyze carbonate content, actual porosity and permeability of the granite, from fresh to highly fractured and veined samples. The location of each measurement is summarized in Fig. 3b.

The main orientation distribution has been plotted in histograms with orientation grouped every five degrees (Fig. 3c). For each group, the veins and fractures have been separated in order to look at the proportion of fractures where paleofluids markers are present. In a general view, all existing fracture directions are partly filled by carbonates and, therefore, opened at least during one stage of crystallization. Also the N070°E direction is the most fractured and, logically, the main direction of the carbonate filled veins. Secondary fracture directions are visible; they all can be linked to faults direction in the regional scale.

The spatial distribution of the fractures on SL1 is shown in Fig. 3c. With all structures in all directions, we observe that the fractures are abundant with a mean density of 24 frac/m, and that there is no influence of the bordering fault located just at the south of the scan line. In contrast, the veins are located in two main density ranges: between 10 and 13 m and between 22.5 and 27 m. To study in more detail this veins distribution, we have decomposed the diagram in accordance with the veins main orientation. The main veins and fractures mapped on the GoogleEarth® view have been added to the diagram. We can see that the two main areas of carbonate precipitation are linked to two different geometries. The first, where the crystallization is at the intersection of major structures even if these structures are not filled by carbonates. The second is the vicinity of the main fault at the outcrop which can be considered as a damaged zone of 3 m on each side of the fault core.

The hand samples have been classified by analogy of the classical model of fault zones (Caine et al., 1996; Faulkner et al., 2010). Four rock facies are distinguished and measured separately with the calcimetry. On one end, the fresh granite where no macroscopic carbonate veins and very few dry fractures are visible. This facies has been measured with 0.3% wt carbonates. On the opposite end, a pure vein that may be compared to a fault core and that was the main host of the paleofluids circulation. The vein sample from the main outcrop fault has 86% wt carbonates, the 14% remaining is composed of few oxydes and granitic breccias. Between these two end-members, we have separated the moderately fractured granite with some macroscopic veins and 2.3% wt carbonates, and the more intensively fractured granite that can be considered as cemented breccias with 32wt % carbonates.

The four facies analysed with calcimetry have been mapped on our fractures map (Fig. 3d). It allows us to distinguish the paeofluids circulation corridors at the meter scale. As seen at the fourth order block scale with the scan line, the most drained area is at the intersection of two fracture directions, between N090° and N070°E, at the northern part of the map. Outside this area we observe drained corridors, mostly in direction N070°E, crossing over the map with other directions that connect the veins network. With each facies mapped, applying the carbonates content measured with calcimetry, we have calculated the wt % represented by each facies on the map (Table 1). The carbonates represent 3.61% of the rock surface. In detail, this are the veins that support the main carbonates crystallization (2.41 wt %) with a significant part located in the breccias area (0.51 wt %).

This study has also been carried out in the area of map 1, located far from the main fault of the block. The calculated carbonate content from map 1 and map 2 (Fig. 3a) is compared in table 1. In summary, we can consider a mean value of 3wt % carbonates in the rock within map 1, that is located far from the main fault, and map 2, that is considered to be in a more drained area. This 3wt% is mostly located in the veins. Only a minor part of the paleocirculation markers is in the host rock, with a percentage almost constant around 0.25.

Finally, porosity and permeability have been analyzed on the hand samples with the same classification of four rock facies (Fig. 3e). The samples can be classified in two groups: 1) represented by all samples of fresh granite and some altered samples, with porosity < 2% and permeability, for the altered samples, varying three orders of magnitude. We can even notice a sample of carbonate vein that is the least permeable due to the entire occlusion of paleoporosity. 2) Group 2 is composed of all the very altered samples and few moderately altered ones, with porosity between 2 and 12%. Permeability varies two orders of magnitude and shows an apparent homogenization with the growth of porosity. However, this last observation must be taken with caution due to the limited number of samples with porosity > 7%.

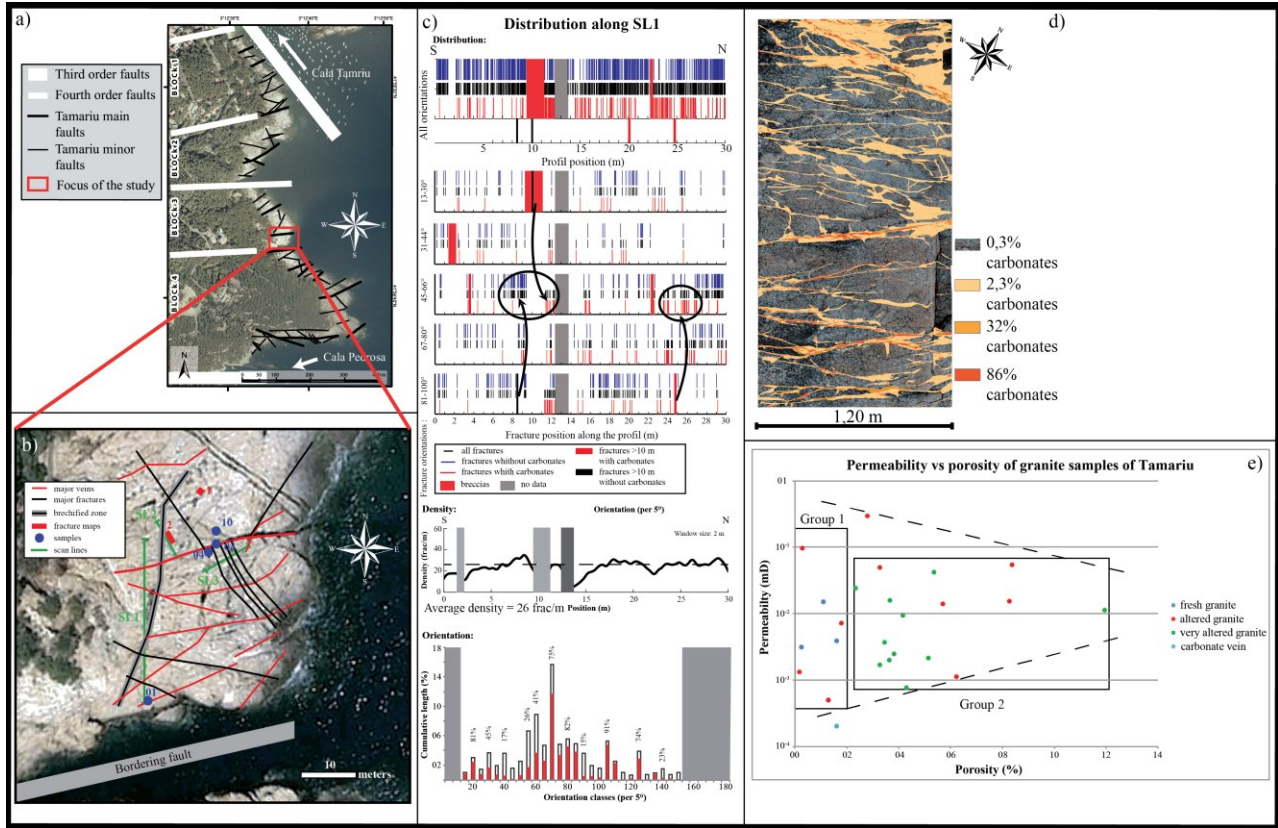


Figure 3: a) Map of Tamariu granite outcropping in the coast with main structures visible at kilometer scale and area of interest for the meter scale study, b) map of the area of interest with location of the measurements and main fractures and veins, c) fractures and veins distribution, density and orientation along the outcrop, d) map 2 example of granite facies with carbonates content, e) Permeability vs porosity of hand samples of each granite facies.

Table 1: Estimation of hydrothermal carbonate content from calcimetry and facies mapping on Tamariu Granite.

	map 2			map 1
	surface (cm ²)	% of carbonates	% of the rock	% of the rock
whole map	28800			
veins	807	86	2,41	2,08
granite breccias	460	32	0,51	0,14
fractured granite	5839	2,3	0,47	0,24
fresh granite	21694	0,3	0,23	0,26
		Total :	3,61	2,72

4. COMPARISON WITH SOULTZ-SOUS-FORET EGs

4.1 Regional scale

The knowledge about the fault network in the Upper Rhine Graben is based on the large seismic campaigns ECORS. These seismic lines highlight three different orders of faults (Fig. 4a). In the first order, there are large faults with roots in the lower crust that structure the basin (red lines, Fig. 4a). They have typical spacing of 8 to 20km and delimit structural blocks like the fractured fields at the basin borders, or the central part of the graben. In the blocks separated by first order faults, there are second order faults that

crosscut the basement and the syn-rift sediments with an average spacing of 4 km, creating a series of tilted blocks (blue lines, Fig. 4a). Finally, third order faults are generally located only in the upper part of the crust, in the sediments giving the system a third order structure (green lines, fig. 4a).

The study of the basement that outcrops in the Northern Vosges Mountains, which is the prolongation of the basement under the URG, allows understanding the faults system in the basement more precisely (Fig. 4b). The map has been drawn with help of the geological maps and the recent review of basement structures (Elsass et al., 2008). On the west side of the first order basin bordering fault, there is a series of second order faults mainly in direction N-S and NW-SE that divide this basement block in second order blocks. The average wide of these blocks is around 2km. Third order faults are visible in some second order blocks suggesting the formation of third order blocks, but the bad exposure of the rocks and the vegetation cover does not allow the precise mapping third order scale faults.

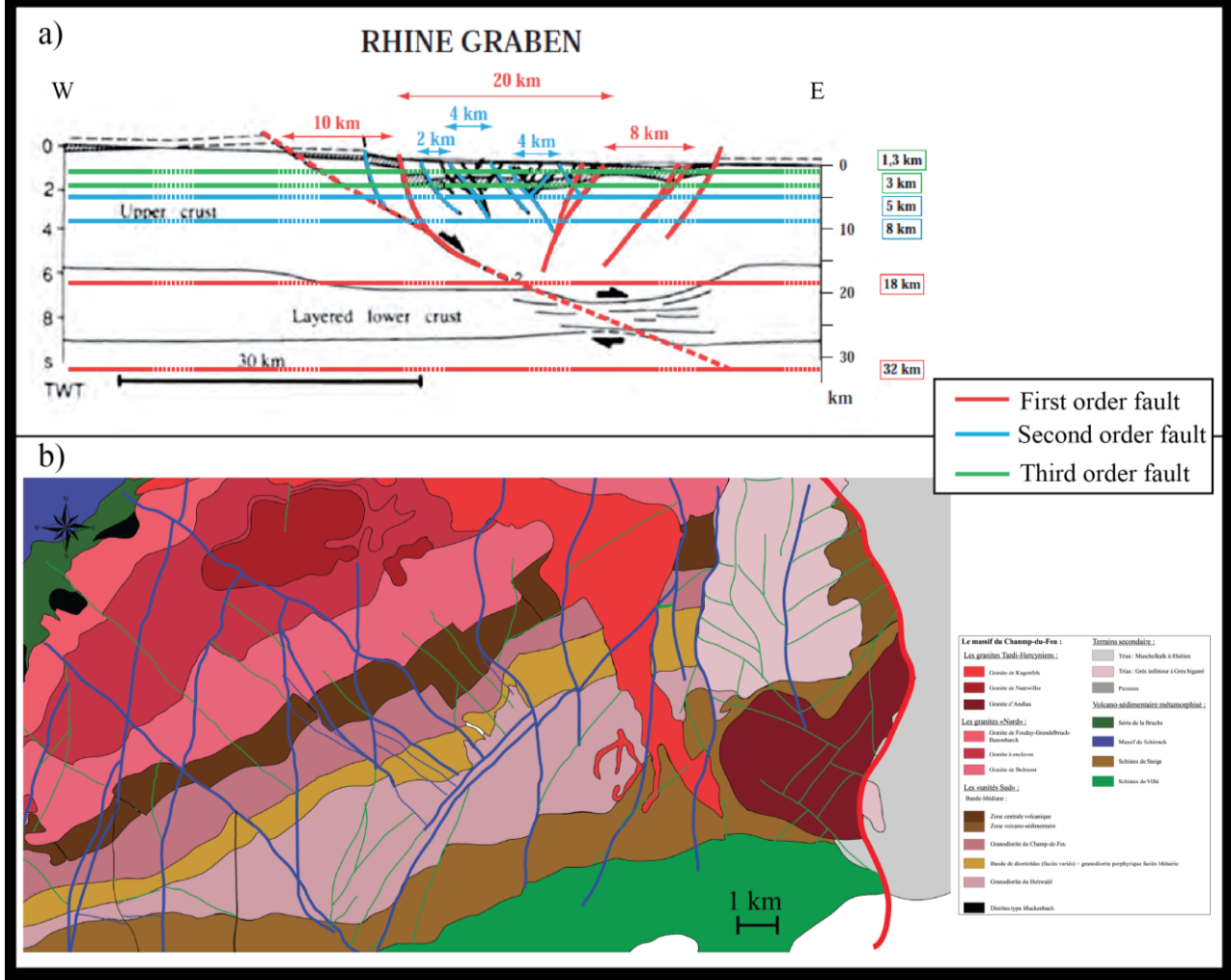


Figure 4: a) Interpretation and schematic view of the ECORS seismic line crosscutting the URG from west to east by Le Garzic (2010), b) geological and structural map of the Northern Vosges Mountains compiled from geological data and Elsass et al. (2008) review.

4.2 Reservoir scale

The Soultz-sous-Forêt EGS is a scientific program started in the 80's aiming to develop knowledge and techniques on geothermal production in deep basement rocks. Its location is at the west of The Rhine Graben, few kilometers away from the graben border, near a highly fractured area called the Savern fractured field. It is composed of one exploration borehole going to 2.2 km depth with 0.8 km in the basement (EPS1), and three production boreholes going below 5 km depth (GPK1, GPK2 and GPK3). The Rhine Graben basement is, at this location, a porphyritic granite dated as Carboniferous (334 ± 3.5 Ma).

The boreholes have been analyzed with image logs based on resistivity contrast of the borehole walls (Fig. 5a). At the granite top, there is a highly fractured zone linked to the alteration of the basement during the Permian and mainly composed of horizontal fractures. These fractures are filled by hematite mineralization. Under this zone, there is an alternation between fractured and better preserved areas. These fractured areas correspond to fault zones that are identified as active for the circulation of geothermal fluids during the hydraulic tests. They have an average spacing between 600 and 1500 m in accordance with the average spacing of third order faults.

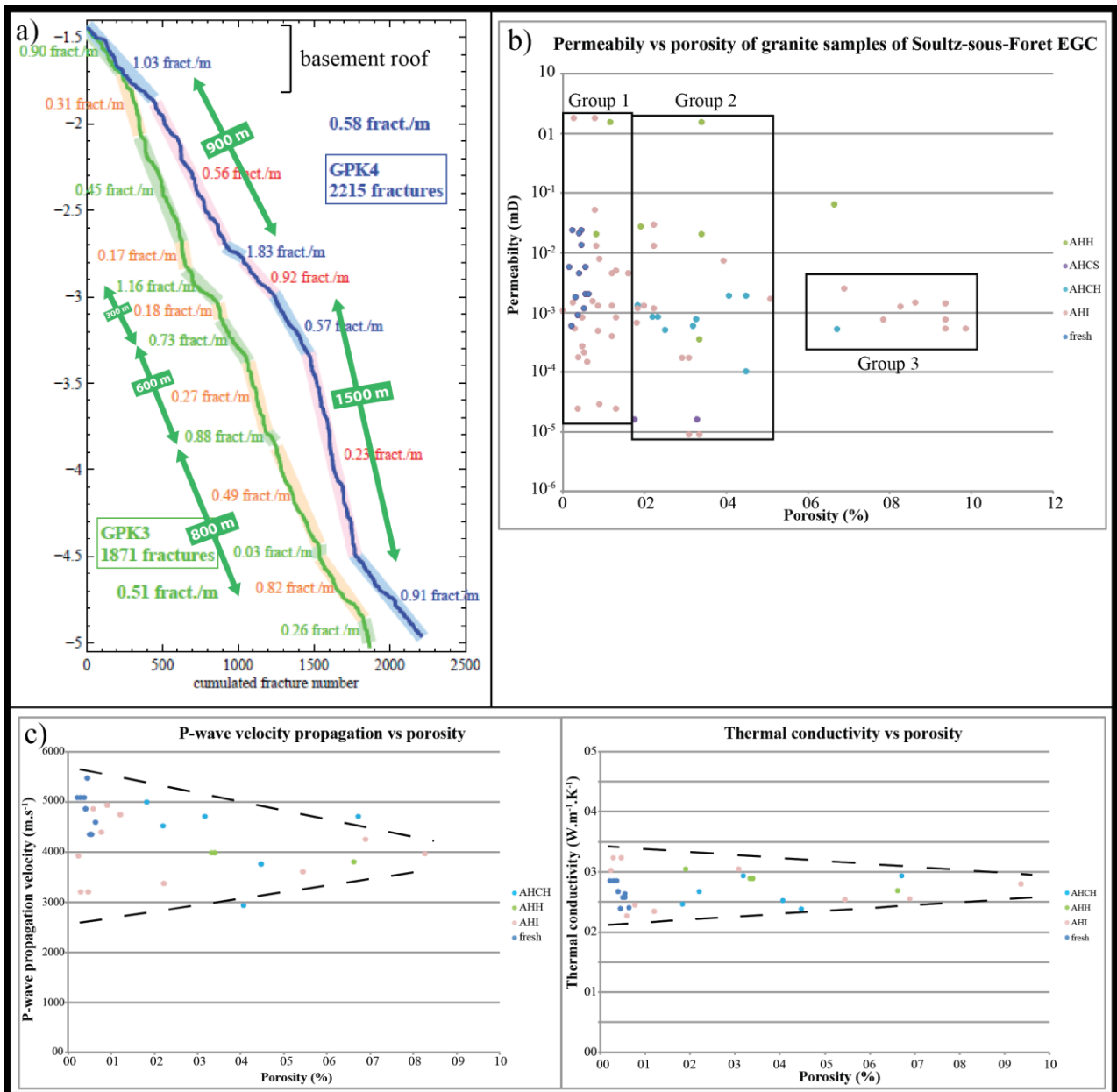


Figure 5: a) Fracture density evolution along GPK3 and GPK4 boreholes analyzed by BHTV modified from Valley (2007), b) permeability vs. porosity and c) P-wave velocity and thermal conductivity vs. porosity of core samples of the different facies of Soultz-sous-Forêt granite.

Aside from the granite top, the fracture filling is mainly composed of two minerals assemblage: 1) a calcite-chlorite assemblage that is homogenously distributed along the borehole resulting from pervasive alteration of the rock groundmass, and 2) a quartz-illite assemblage that is localized in the fault zones and results from preferential paleofluid flow through these faults (Le desert et al., 2009). In addition, the rock matrix has been subjected to different stages of alteration leading to the classification of the granite in five facies (Rosener, 2007):

- Fresh granite
- AHC : granite hydrothermally altered with red K-feldspar and plagioclase partly replaced by chlorite
- AHI : granite hydrothermally altered with K-feldspar surrounded by secondary plagioclase, primary plagioclase replaced by illite and highly altered biotite
- AHH : granite hydrothermally altered with altered plagioclases filled by hematite.
- AHCH : the same hydrothermal alteration of AHH with high microfracture density.
- AHCS : granite with grain reduction linked to the hydrothermal alteration and fracturing, and secondary quartz and illite.

Samples taken at different depths from the cores of EPS1 have been measured in porosity, permeability, thermal conductivity and P-wave velocity. From the microscopical structures and alteration degree, and the permeability and porosity values, three groups of sample have been identified (Fig. 5b). The group 1 is composed of all samples of fresh granite and the less altered AHI and AHH with less than 2% porosity and extremely variable permeability (10^{-5} mD to few mD). On these samples, the porosity is mainly composed of microfractures and the permeability is directly linked to the density and connectivity of these microfractures. Group 2

is composed of samples of AHI, AHH, and most samples of AHCH and AHCS, with porosity between 2 and 5% and the same variability of permeability than group 1. In the samples, there is influence of both microfractures and secondary minerals due to matrix alteration. Group 3 is formed by the most porous samples, up to around 10% porosity, is mainly composed of AHI facies and the permeability is more even around 10^{-3} mD. In fact, in these samples the matrix alteration is high enough to create a connected porous network that completely hides the effect of the microfractures.

Thermal conductivity and P-wave velocities have been plotted against porosity (Fig. 5c). These two properties are dependent on mineralogy, porosity and pore space geometry. For P-wave velocity, the primary minerals have globally the same velocities (around $5000 - 6000$ m.s $^{-1}$) and are in good correlation with the fresh granite samples. In contrast, the secondary minerals, more precisely clays, expose lower velocities that change the whole material's velocity. Furthermore, the variability of P-wave values of the less porous samples can be attributed to the development of the microfractures, while the homogenization of velocity for the most porous samples is due to the important influence of the secondary minerals and associated porosity. For the thermal conductivity the effect of alteration and porosity increase is, in general, the same. Nevertheless, a less pronounced heterogeneity is observed for less porous samples.

5. DISCUSSION AND CONCLUSIONS

The Catalonian Coastal Ranges and the Upper Rhine Graben are both deeply linked to the geological history of the Hercynian orogeny and the West European Rift event. According to that, we have analyzed each area from the regional scale to the microscopical scale in order to compare them. Keeping in mind some differences between the two areas, the Catalonian Coastal Ranges is a useful analogue for the comprehension of the Soultz-soultz-Forêt EGS and, more generally, for basement reservoirs in extensive settings. These differences are: the Catalonian Coastal Ranges is an outcrop and provides horizontal information about the rock structures, whereas the Soultz-sous-Forêt data is vertical, and this information needs to be corrected for burial effects for exploitation in real reservoirs cases. In addition, there is the influence of the Catalonian transform fault that is not present in the Upper Rhine Graben.

On the regional scale, the study of the CCR has allowed the classification of faults in different orders of scale, and to deduce the main characteristics of the fault system like spacing, length, width, orientation distribution at different scales of observation (Fig. 6a). Therefore, we can notice that these parameters do not have the same behavior at different scales: some of them, e.g. orientation, are dependent on the observation scale, and others, e.g., length, are homogenous from the hundred kilometers to the centimeter scale. With the rapid observation of the E-W crosscut of the URG and the Vosges Mountain map, we recognize the same order of scales for the faults and blocks. Thus, behavior of the fault parameters of the CCR can be extrapolated to the URG allowing completion of the information obtained by the geophysical data of the URG.

Between each scale of observation there is an evolution of the apparent fault morphology. In fact, each fault at one scale is a cluster of faults at a smaller scale (Fig. 6b), with characteristic spacing and thickness of the clusters at each scale. Consequently, at borehole scale in the Soultz-sous-Forêt EGS, third and fourth order scale faults are not directly visible but are represented by an increase of the fracture density visible in the borehole images. Therefore, to obtain information of the reservoir in 2D and 3D, the study of Tamariu at reservoir scale in the CCR is a useful tool. The observation of the fracture network in a fourth order block with the help of paleocirculation markers on Tamariu allows the identification of the main circulation corridors: the intersection of the main fracture direction and the damage zone of faults crosscutting the blocks.

The quantification of the carbonate markers on Tamariu gives information about the paleovolume available for fluid flow in the inner part of a fourth order structural block. Even though the alteration phases seem more complex on Soultz-sous-Forêt granite with the different facies AHI, AHH, AHC for altered rocks and AHCH and AHCS for fractured and altered rocks, the petrophysical evolution from fresh to highly altered granite are analog for the two batholiths. In fact, we have noticed high variation of permeability for samples with porosity lower than 2 % suggesting a large control of the microfracture density, and a global homogenization of the permeability with the increase of porosity, and hence the alteration and formation of secondary minerals in the rock matrix. This alteration seems to completely remove the effect of the microfractures heterogeneity for porosities higher than 6 %.

In a third order block available for geothermal production, we can use the fracture data to estimate the internal division in fourth order blocks, with centimeter to hectometer scale faults and fractures creating a connected network for the fluid flow. These fractures and faults control the temporal and spatial evolution of the alteration and permeability of the rock mass (Fig. 6c). The highest porosity is in the damaged zone at the different scales, with matrix permeability 3 to 5 orders of magnitude higher than in the protolith. However, in the fault cores and most altered areas the permeability and porosity are not optimal with clays preventing the development of higher permeability, thus potentially decreasing the matrix porosity.

REFERENCES

Arthaud, F., Matte, Ph. : Les décrochements tardi-hercyniens du Sud-Ouest de l'Europe, géométrie et essai de reconstitution des conditions de la déformation. *Tectonophysics* **25**, (1975) 139-171.

Bertrand, L., Le Garzic, E., Place, J., Géraud, Y., Diraison, M., Walter, B., Haffen, S.: A multiscale analysis of the fracture pattern in granite: A case study of the Tamariu granite, Catalunya, Spain, in review.

Brun, J.P., Wenzel, F.: Crustal-scale structure of the southern Rhinegraben from ECORS-DEKORP seismic reflection data. *Geology* **19**, (1991), 758-762.

Caine, J.S., Evans, J.P., Forster, C.B.: Fault zone architecture and permeability structure. *Geology* **24**, (1996), 1025-1028, doi: 10.1130/0091-7613.

Cautru, J.P.: Coupe géologique passant par le forage GPK1 calée sur la sismique réflexion, et documents annexes. Document interne IMRG, GEIE «Exploitation Minière de la Chaleur», Kutzenhausen, France, (1989).

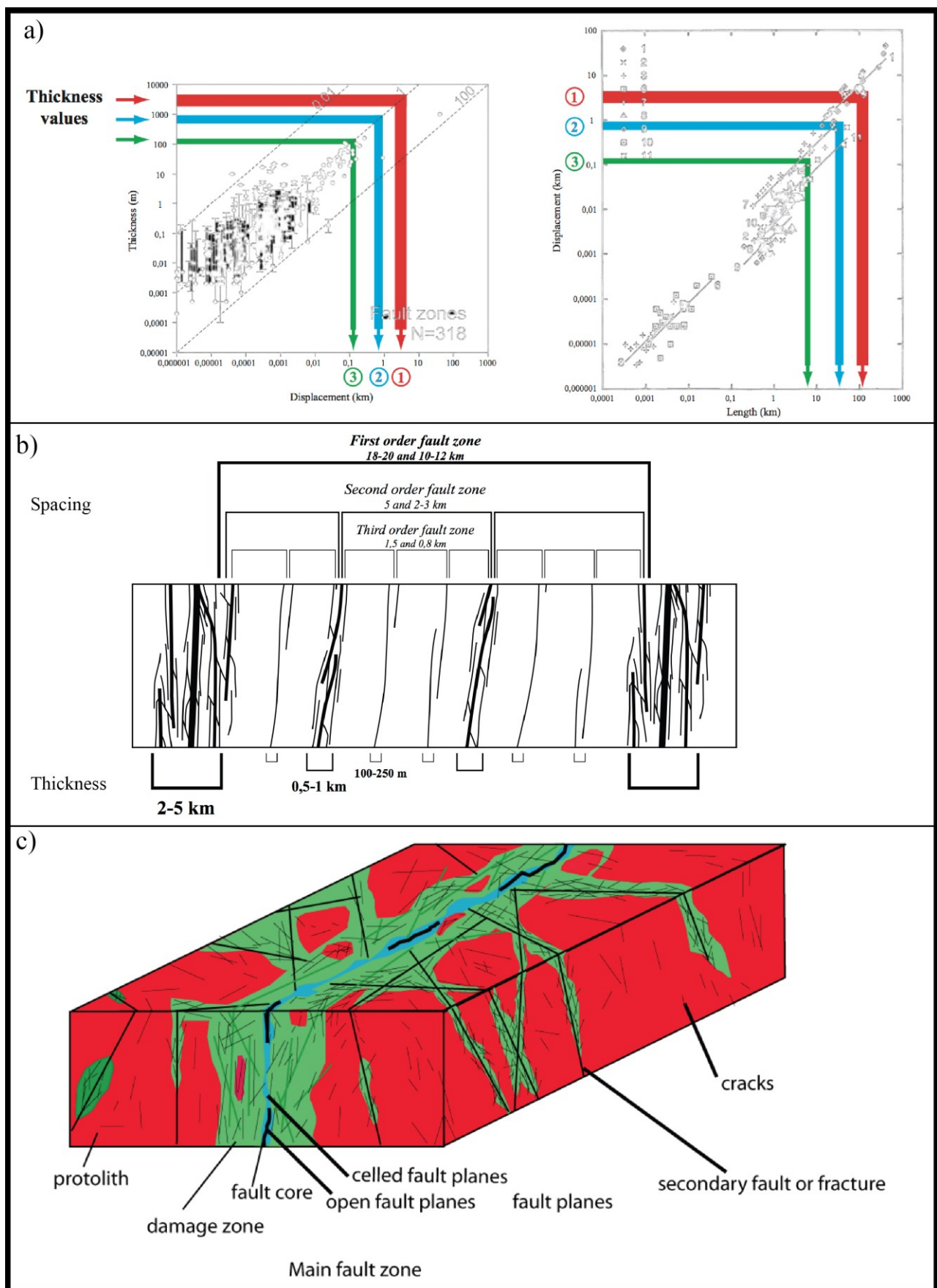


Figure 6: a) Estimation of faults displacement and length of three order scales with their thickness and general laws by Le Garzic (2010) modified from Childs et al. (2009) and Clark and Cox (1996), b) model of faults scaling for basement in extensional settings by Le Garzic (2010), c) synthetic model of porosity and permeability facies distribution in the basement.

Childs, C., Manzocchi, T., Walsh, J.J., Bonson, C.G., Nicol, A., Schöpfer, M.P.J.: A geometric model of fault zone and fault rock thickness variations. *Journal of Structural Geology* **31**, (2009), 117-127.

Clark, R.M., Cox, S.J.D.: A modern regression approach to determining fault displacement- length scaling relationships. *Journal of Structural Geology* **18**, (1996), 147-152.

Elsass, P., Von Eller, J.P., Stussi, J.M.: Géologie du massif du Champ-du-Feu et de ses abords. Eléments de notice pour la feuille géologique 307 Sélestat. Rapport BRGM RP-56088-FR (2008).

Faulkner, D.R., Jackson, C.A.L., Lunn, R.J., Schlische, R.W., Shipton, Z.K., Wibberley, C.A.J., Withjack, M.O.: A review of recent developments concerning the structure, mechanics and fluid flow properties of fault zones. *Journal of Structural Geology* **32**, (2010), 1557-1575.

Genter, A., Guillou-Frottier, L., Feybasse, J.L., Nicol, N., Dezayes, C., Schwartz, S.: Typology of potential Hot Fractured Rock ressources in Europe. *Geothermics*, **32**, (2003), 701- 710.

Le Garzic, E.: Distribution multi-échelle de la fracturation dans les réservoirs cristallins, influence de l'héritage strcutural. In : PhD thesis. University of Strasbourg, France, (2010), 268 pp.

Place, J., 2010: Caractérisation des chemins de circulations de fluides dans le réseau poreux d'un batholite granitique. In: PhD Thesis, University of Strasbourg, France, (2010), 360 pp.

Roca, E., Sans, M., Cabrera, L., Marzo, M.: Oligocene to Middle Miocene evolution of the central Catalan margin (Northwestern Mediterranean). *Tectonophysics* **315**, (1999), 209–233.

Rosener, M.: Etude pétrophysique et modélisation des effets des transferts thermiques entre roche et fluide dans le contexte géothermique de Soultz-sous-Forêts. PhD Thesis, University of Strasbourg, (2007), 207pp.

Séranne, M.: The Gulf of Lion continental margin (NW Mediterranean) revisited by IBS: an overview. In: Durand B., Jolivet L., Horváth F., Séranne M., (Eds.). *The Mediterranean Basins: Tertiary extension within the Alpine Orogen*. Geological Society, London, Special Publications **156**, (1999), 15-36.

Skrzypek, E.: Contribution structurale, pétrologique et géochronologique à la tectonique intracontinentale de la chaîne hercynienne d'Europe (Sudètes, Vosges). PhD Thesis, University of Strasbourg, (2011), 416pp.

Thabaud, A.S.: Le magmatisme des Vosges : conséquence des subductions paléozoïques (datation, pétrologie, géochimie, ASM)? PhD Thesis, University of Strasbourg, (2012), 231 pp.

Valley B.C.: The relation between natural fracturing and stress heterogeneities in deep-seated crystalline rocks at Soultz-sous-Forêts (France). PhD thesis, University of Zurich, (2007) 297 pp.